J. Condensed Matter Nucl. Sci. 23 (2017) 27–44

Research Article

Simulation of the Behavior of Exotic Neutral Particles by a Monte-Carlo Modelisation

Jacques Ruer*

Abstract

Hot spots are small features that some authors suppose are created by a sudden local release of thermal energy. For example, the estimation of the energy involved in the formation of a 2 μm crater is 3×10^{-8} J or 2×10^{5} MeV. Some theories attempting to explain these phenomena, and excess heat in general, involve the role of Exotic Neutral Particles (ENP), like Polyneutrons or Erzions. According to such theories, these ENPs are relatively rare. The problem investigated in this paper is whether a single particle may trigger a series of many reactions within a short time in solids that are properly loaded. A Monte-Carlo simulation has been written to study the potential behavior of ENPs. It is shown that the ENPs follow a developed and Brownian type movement. The number of reactions occurring at a given depth below the surface is calculated, as well as the probability for a series to exceed a given value. From a pure mathematical viewpoint, a parallel can be made between the diffusion laws and Brownian motion. It is shown that a small fraction of the ENP flux can trigger large series of reaction, to the point that the energy that can be produced is not limited if the ENP is stable as long as it is present in the lattice. It is necessary to introduce a limited lifetime with a decay to reconcile the model with the experimental observations. The discussion of the simulation results in the light of experimental data leads me to propose a mean free path on the order of 100 Å, and a lifetime in the nanosecond range.
 ISSN 2227-3123

Keywords: Brownian motion, Exotic neutral particles, Hot spots, Monte-Carlo, Particle lifetime, Simulation

1. Introduction

Low Energy Nuclear Reactions (LENR) are thought to be responsible for the generation of excess heat in some experimental conditions. Positive experimental results have been obtained in many instances. This form of energy could prove immensely important in the future, but the lack of a comprehensive theory of the phenomena impedes the development.

LENR are difficult to explain if we base the theoretical analysis on classical physics. Many theories have been proposed to explain how atoms could fuse at relatively low temperatures [1,2].

Among these theories, one category involves the role of hypothetical particles that could lower the energy barrier between atoms and make reactions possible. The Polyneutron theory proposed by Fisher [3,4] proposes that neutrons are exchanged between nuclei.

*E-mail: jsr.ruer@orange.fr.

 ISSN 2227-3123

Bazhutov [5,6] supposes the existence of a hypothetical particle called Erzion, which could lead to a similar effect. Collis [7–9] remarks that these theories share common features and proposes the name Exotic Neutral Particle (ENP) to describe them. He thinks that the rates of reaction are expected to be very high, permitting a tiny number of ENPs to create substantial heat and transmutation products.

The purpose of this paper is to follow up on this basic idea and investigate some of the properties ENP would require to be able to describe the phenomena observed.

2. LENR Effects

LENR phenomena have been confirmed in different kinds of experimental setups, from electrolysis to gas phase reactors [1]. The excess power is reported to be sometimes as high as 1 $\mathrm{W\,cm^{-2}}$. In some cases, the surface of the samples exhibits small features looking like tiny craters [10,11]. Figure 1 shows an example of craters. Some authors think that violent reactions caused the melting of the metal during the formation. If this is the case, it can be demonstrated that the crater formation is very rapid [12]. The energy required to create a crater has been estimated. For example, a crater with a diameter of 2 μm corresponds to an energy of 2×10^{-9} J, released in about 6×10^{-9} s. In other cases, hot spots have been detected with infrared cameras [10].

It can be calculated that the energy released during the formation of craters and hot spots is only a small fraction of the excess heat measured from samples during positive experiments. This means that besides localized energy, a large fraction of the energy is generated in a diffuse manner without leaving apparent traces.

This paper does not analyze the detailed mechanism of the reactions involving ENPs. The purpose is rather to examine how ENPs could produce sufficient quantities of energy to explain the observed phenomena. A model is presented which attempts to describe the statistical behavior of the ENPs, and to find out what the properties of these hypothetical particles should be in order to explain the experimental results.

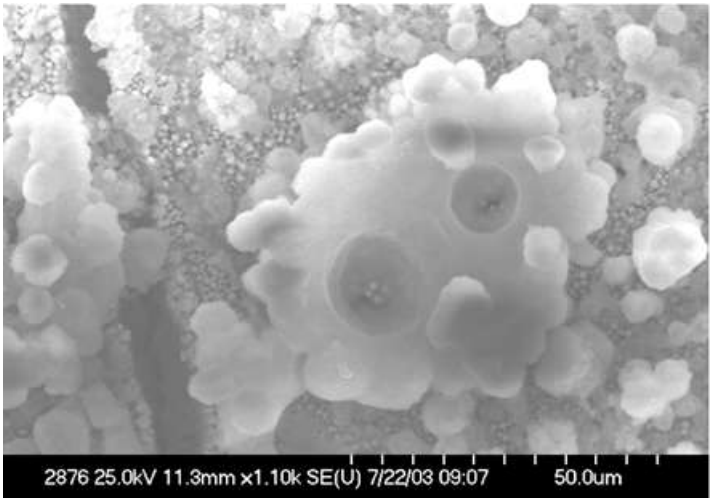

Figure 1. Example of craters observed after co-deposition experiment [10]. The rounded shape of the voids and the debris around the rim suggest that metal was melted during the formation of the craters.

3. Simulation Model

In order to develop a better understanding of the problem, a simple Monte-Carlo type model has been developed and written. The model assumes as a starting point that ENPs exist and are responsible for the LENR phenomena. The objective of the simulation is to compare mathematical results with the experimental results, in an attempt to develop some arguments in favor or against ENP theories. For instance, should the simulation lead to some contradiction between the hypotheses and the results of the simulation, the theory might have to be rejected. We see in the following that this is not the case. However, it is demonstrated that the ENPs should have specific properties to reconcile model and experimentation.

Assuming that ENPs are at the origin of the heat, the model must take into account the following assumptions:

- ENPs are deemed relatively rare. The logical consequence of this assumption is that a single particle should be able to trigger a series of many reactions within the metal lattice. One ENP is not destroyed by the reactions but remains available for further reactions, at least for some time.
- Some of the ENPs must remain a sufficient time to develop the quantity of energy corresponding to a hot spot or a crater.

3.1. Hypotheses

The following set of hypotheses {H} is taken into consideration to elaborate the simulation model. Figure 2 shows a sketch of the model:

- H1: The metal lattice, properly loaded and processed is reactive, so that the ENPs interacting with the lattice trigger LENR reactions.
- H2: One ENP enters the metal and triggers a first reaction at a given depth below the surface Z_0. This depth may be zero.
- H3: After a reaction, the ENP retains its capacity to trigger further reactions.
- H4: The ENP travels along a straight line in the metal lattice until it reacts again.

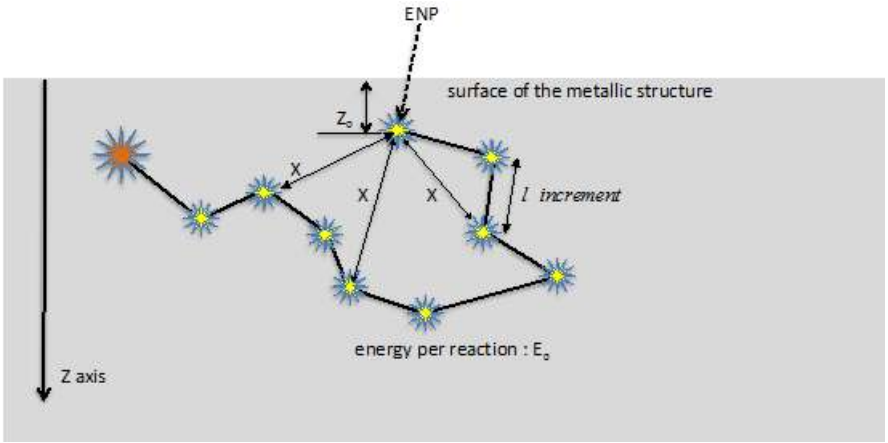

Figure 2. Sketch of the model – The ENP (origin unknown) starts to react at a depth Z_0 under the surface (Z_0 may be zero) – It travels at random in the lattice, triggering reactions at some spots – The activity stops if the ENP leaves the lattice, or after a given number of reactions Λ.

- H5: To simplify the model, all the reactions are assumed to be of the same nature and to release the same energy E_0.
- H6: The direction of the velocity vector after a reaction may be completely independent of the velocity before the reaction, or this new vector may be compounded with a fraction of the vector before the reaction.
- H7: If the ENP trajectory again crosses the metal surface, the ENP is lost in the environment and the series of reactions is interrupted.
- H8: In the simulation, the series are limited by a maximum number of reactions, called the Life Number: Λ. This life number proves to be a governing factor for the overall behavior, as explained hereafter.
- H9: The space increment is given by a classical absorption exponential law [13]. The probability that a particle will travel at least a length l is represented by the equation:

$$P(l) = \mathrm{e}^{-l/L_0}. \tag{1}$$

According to this equation, the mean free path is L_0.

3.2. Basic assumptions

Three main unknowns can be identified in the simulation:

(1) The value of the mean free path L_0.
(2) The average time lapse between successive reactions, which depends on the travel time along L_0 and of the reaction time itself of the excited compound. At this stage of the study, we suppose that the reaction time is zero. The moving velocity U of ENPs within the lattice is a parameter that is not known and needs to be evaluated.
(3) The quantity of energy E_0 released by a single reaction. For the purpose of this simplified simulation, a precise value is not critical. According to the theories, not all reactions are alike, and the energies are different [2–9]. In this simulation, only an average value is required. We use, quite arbitrarily, an average energy of $E_0 = 4$ MeV per reaction. With this hypothesis, the formation of a 2 μm crater would correspond to 50 000 reactions.

3.3. Description of the model

The model is a Monte-Carlo simulation that operates as follows:

- One ENP is first located at the depth Z_0.

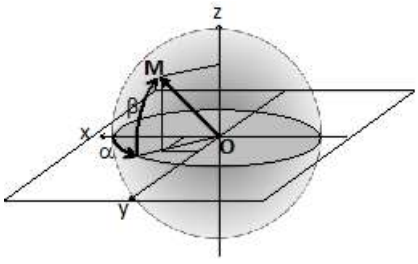

Figure 3. Generation of a new velocity vector OM.

- The three components of the new velocity vector are generated using two different pseudo-random number generators PRNG#1 and PRNG#2 (see Fig. 3). The method used to generate the random numbers is presented in the Appendix.
- The mean free path in the mathematical model is unity, by convention. The length l of the space increment between successive reactions is given by a third pseudo-random number generator PRNG3:

$$C_n \in [0\,,\,1] \quad \text{value from pseudo-random generator } \#3,$$

$$l = -\text{Log}(C_n). \tag{2}$$

- The new velocity vector may be compounded with a fraction of the old vector before the reaction, to take into account the conservation of the momentum in the interaction, should the ENP have a mass different from zero.
- The reactions are counted. The statistical distribution of the reactions around the introduction site is calculated. This makes it possible to evaluate the spatial distribution of the energy.
- The series of reactions for a given ENP is interrupted by one of the following events:
  - The ENP is located at a negative depth (escape out of the metal).
  - The number of reactions reaches the predefined Λ value.
- A new ENP is introduced and the simulation proceeds.
- In order to obtain representative statistical results, a large number of ENPs is used, from 10^5 to 10^7.

$$A_n \in [0\,,\,1] \quad \text{value from pseudo random generator } \#1,$$

$$B_n \in [0\,,\,1] \quad \text{value from pseudo random generator } \#2,$$

$$\alpha = 2\pi A_n, \quad \alpha \in [0\,,\,2\pi]\,,$$

$$b = 2B_n - 1, \quad b \in [-1\,,\,+1]\,,$$

$$\beta = \sin^{-1}(b), \quad \beta \in [-\pi/2,\,+\pi/2]\,.$$

New velocity vector components:

$$V_x = \cos\alpha \cos\beta,$$

$$V_y = \sin\alpha\, \cos\beta,$$

$$V_z = \sin\beta.$$

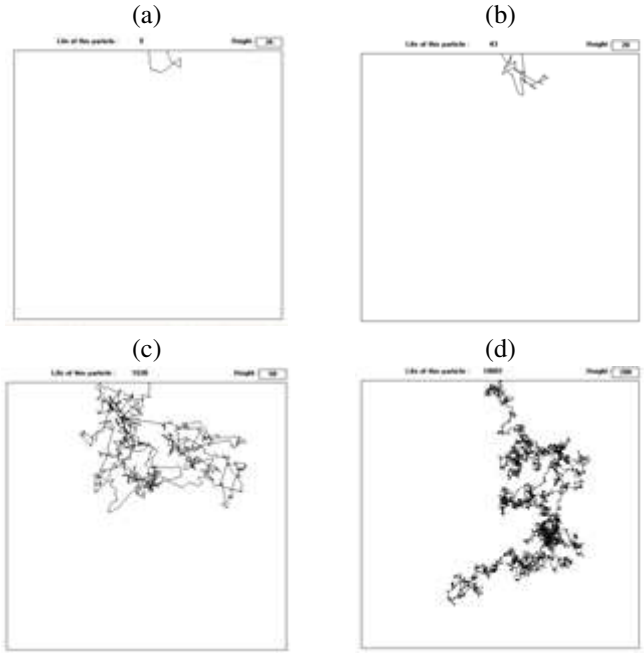

Figure 4. Typical examples of trajectories – Most ENPs give a small number of reactions (Fig. 4a or 4b). Only exceptional cases give long series (Fig. 4c or 4d) – Life numbers are, respectively 9, 43, 1038, and 10 001 – Please note that the different scales (Heights: 4a = 20, 4b = 20, 4c = 50, and 4d = 200 mean free paths).

4. Brownian Motion

This kind of simulation results in a random trajectory of the ENP. Some examples are shown in Fig. 4. They are typical of Brownian motion.

The above pictures display the trajectories of some individual ENPs. If we follow the behavior of many particles introduced at the same site, we obtain the statistical spatial distribution of the reactions, or the spatial distribution of the energy released. Figure 5 shows a typical result. One can see that for $Z_0 = 0$ the average energy distribution is contained in spheres tangent to the surface at the introduction point.

The mathematical definition of Brownian motion is the fact that the mean value of the squares of the excursions X (Eq. (3)) is proportional to the time [14,15]. Figure 2 illustrates the meaning of X. The distance, or excursion, travelled since $t = 0$ is measured in the $3d$ space, or projected along one direction ($d = 1$). We write Eqs. (3) and (4)

$$\langle X^2(t)\rangle = \frac{1}{t}\int_0^t X^2\,(t)\,, \tag{3}$$

$$\langle X^2(t)\rangle = dDt, \tag{4}$$

where X is the excursion of the particle at time t, d the dimensionality of the configuration ($d = 1$ for a 1-dimension diffusion problem and $d = 3$ for a 3-d space) and D is the diffusion coefficient.

Diffusion coefficients are measured in m^2s^{-1}. The model utilizes a length unit (L_0), which is unknown, and does not take the time into account. So, it can only verify the type of relationship, rather than the diffusion coefficient itself.

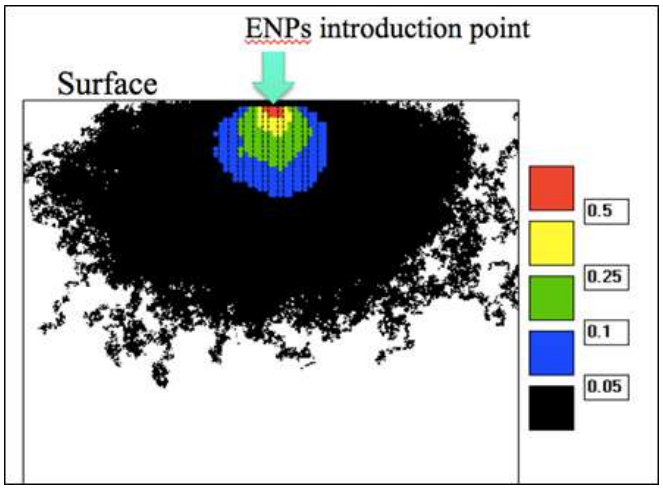

Figure 5. Spatial distribution of the reactions with many particles introduced at the same point on the surface. Result obtained with 10^5 particles - Life Number $\Lambda = 10^4$ - In this picture, the number of reactions are computed in a grid of 100×100 elements perpendicular to the surface. The third coordinate perpendicular to the plane of the picture is not monitored (all reaction spots are projected on the grid plane). The size of a grid element is $5L_0$. The color scale shows the ratio of the number of reactions in one grid element to the peak one in the grid element located just below the introduction point.

Figure 6 shows the results obtained by the model. The relationships between $\langle X^2 \rangle$ and the number of reactions n are

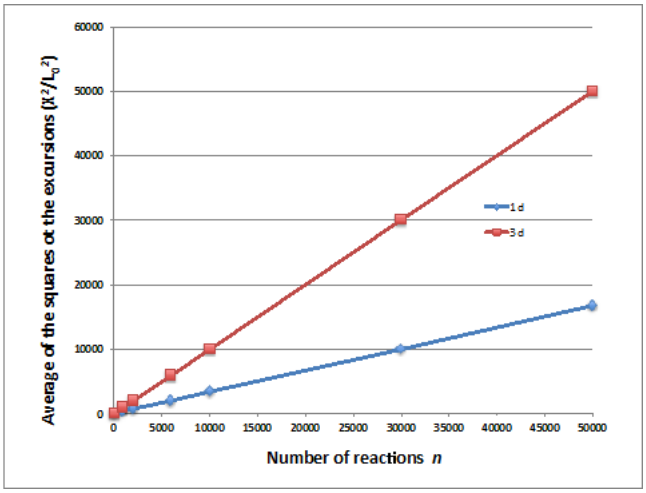

Figure 6. Results of simulations – Relationship between the number of reactions and the average square values of the excursions – For these calculations, Z_0 has been deliberately chosen very high so that no ENP could escape even for high life numbers Λ. All series have a number of reactions n equal to Λ. Equivalent diffusion coefficient $\Delta = 0.33$ in 1d and $\Delta = 1.0$ in 3d.

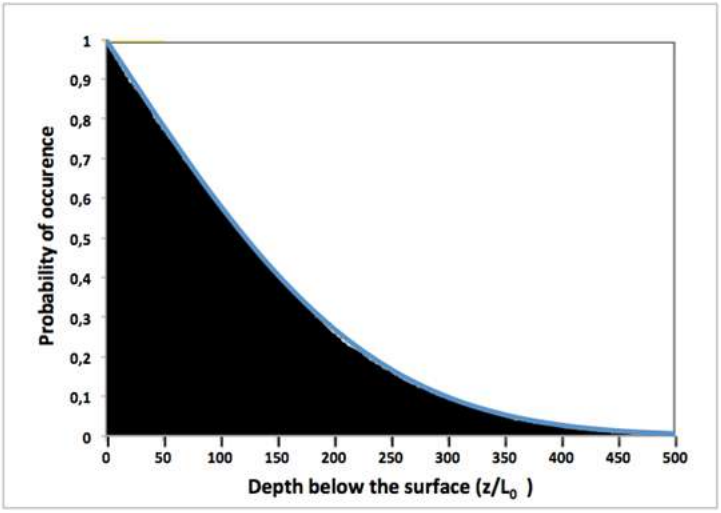

Figure 7. Comparison between the probabilities of occurrence calculated by the simulation and application of the second Fick's law – simulation with 10^6 particles and $Z_0 = 0$, Life Number $\Lambda = 50\,000$, and $\Delta = 1/3$.

linear, both in 1d or 3d, typical of Brownian motion:

$$\Delta = \frac{\langle X^2 \rangle}{nd}. \tag{5}$$

The value of the proportional constant is:

$$\Delta = 0.33 \quad \text{for } d = 1 \text{ along the } z\text{-axis},$$

$$\Delta = 1.0 \quad \text{for the spatial diffusion } (d = 3).$$

It is known in the literature that a duality exists between Brownian motion and the diffusion described by Fick's equations [16]. The same behavior is found here again. Figure 7 compares the statistical presence of the ENPs at different depths obtained by application of the classical diffusion laws to the distributions given by the model for $Z_0 = 0$.

The statistical distributions of the model can be fitted with the curves (*in blue*) given by the equation, similar to the second Fick's law of diffusion:

$$C(z, n) = a \left[1 - \operatorname{erf} \left(\frac{z}{2\sqrt{\Delta n}} \right) \right]. \tag{6}$$

5. Statistical Results of the Simulation

5.1. Simulations with $Z_0 = 0$

The probability of occurrence of ENPs decreases as a function of depth. Most of the events are close to the surface. However, for large Λ values, the occurrence of ENPs at depths as large as a few hundreds of mean free paths is possible (see Fig. 7). When $Z_0 = 0$, half of the ENPs escape at the beginning of the sequence (see, e.g. Fig. 4a and b). On the other hand, some ENPs remain within the metal up to Λ, whatever its value.

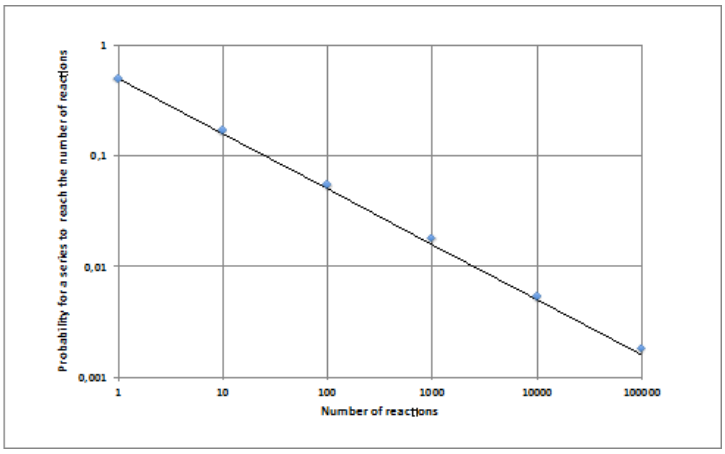

Figure 8. Proportion of particles still present under the surface after a given number of reactions – Calculations made with 10^5 particles – $Z_0 = 0$ – The line corresponds to Eq. (7).

Figure 8 shows the distribution of the probability for a particle to reside in the metal during a series of a given length. The graph uses logarithmic coordinates. It indicates that the probability that a series will reach a given number of reactions N is well approximated by the equation:

$$P(N) = 0.5 \times N^{-0.5}. \tag{7}$$

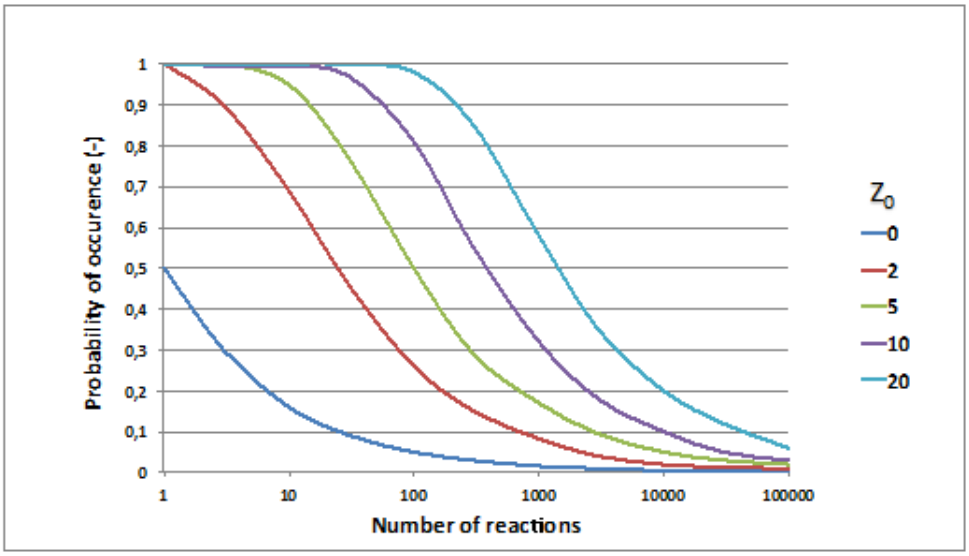

Figure 9. Distributions of probabilities for different Z_0 values.

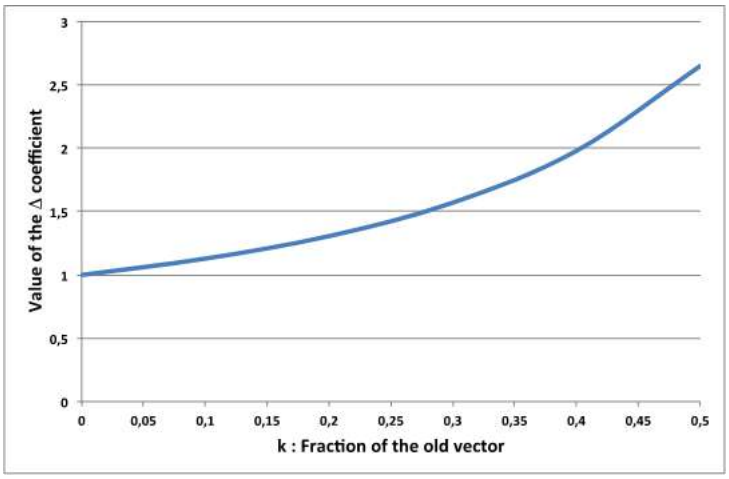

Figure 10. Influence of the compounding of the velocity vectors on the Δ coefficient.

5.2. Simulations with $Z_0 > 0$

If the first reaction takes place below the surface, the probability of observing a long series is greatly enhanced. Figure 9 shows the distributions of the probabilities to reach a given number of reactions for different Z_0 values.

It can be seen that the probability of a large series is increased even for modest Z_0 values. This is an important result, as shall be discussed below.

5.3. Simulations with compounded velocity vectors

The simulation can take into account a combination of the new velocity vectors after the reaction with a fraction of the velocity before the reaction. This combination represents the effect of the conservation of the momentum of the particles during the interaction. The value of k depends on the relative masses of the ENP and the atoms that are reacting.

$$\overrightarrow{V_r} = \left(k \cdot \overrightarrow{V}_{\text{old}} + \overrightarrow{V}_{\text{new}}\right). \tag{8}$$

The effect of the compounding is an increase in the diffusion coefficient Δ. Figure 10 shows the relationship between k and Δ.

The mass of the ENP is unknown. This simulation indicates that the influence of a mass greater than zero does not change the behavior to a great extent. The only effect is to increase the diffusion coefficient. The same effect would be obtained by the simulation with $k = 0$ and a mean free path equal to:

$$L = \sqrt{\Delta}\ L_0. \tag{9}$$

In the following, L is called the equivalent mean free path.

6. Discussion of the Results

It can first be remarked that most series end up with a modest value of the number of reactions. Such series could correspond to the majority of the events that contribute to the generation of heat but leave no traces on the samples.

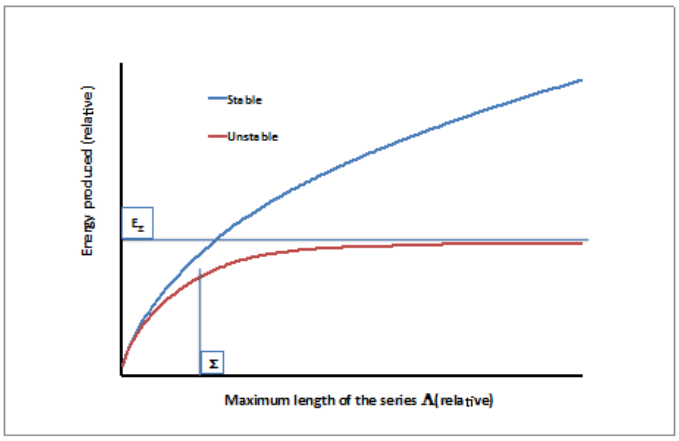

Figure 11. Schematic comparison of the energy released by stable and unstable ENPs. If ENPs are stable, there is no limit to the energy if there is no limit to Λ. If the ENPs are unstable, the energy converges to an asymptotic value for large reaction numbers Λ.

However, some series reach Λ, whatever its value. This is an essential result, because the major share of the energy released is created by the large series, as shown here. Let us consider again the occurrence probabilities calculated by Eq. (7).

The average energy produced by ENPs with a lifetime Λ can be calculated by the equation:

$$E = E_0 \int_0^{\Lambda} P(n)\, \mathrm{d}n. \tag{10}$$

We obtain

$$E = E_0\, \Lambda^{0.5}. \tag{11}$$

This equation gives a diverging result. If there is no limit to Λ, there is no limit to the average energy produced! This does not correspond to experience. Therefore, we must admit that Λ is limited for some reason. Potential phenomena able to provide the limitation are listed here. This list is probably not exhaustive.

- The energy locally increases the temperature. The lattice may lose its reactivity when the temperature is too high.
- The lattice may be active only in small spots. When the ENP leaves this active zone, it does not trigger additional reactions, even if it is present in the lattice, in an inactive area.
- The ENP may lose its properties prematurely.

Among these hypotheses, the last one is interesting. We may suppose that the ENP is unstable. Let us suppose that the ENP follows a decay law similar to radioactive elements. We write the probability of the presence of the ENP as

$$Q(t) = \mathrm{e}^{t/T}, \tag{12}$$

where T is the time constant of decay. The number of reactions is proportional to the time of presence, so that we can define a mean life number Σ, and the number of reactions during the time T. Equation (12) may be replaced by the

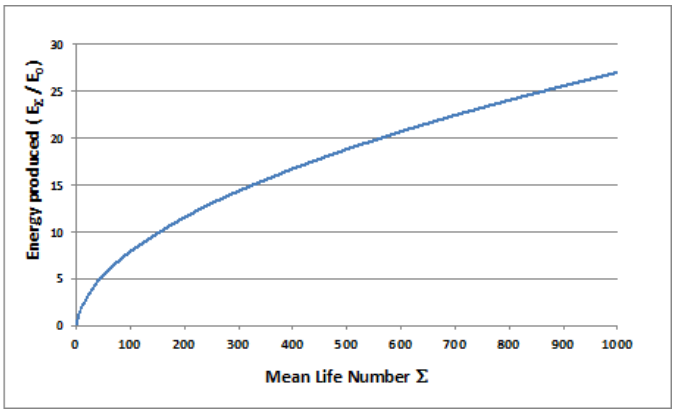

Figure 12. Relationship between Σ and E_Σ.

equation:

$$Q\,(N) = \mathrm{e}^{-N/\Sigma}. \tag{13}$$

With this additional hypothesis, the probability that a series will reach the number of reactions N is the product of the probability of the series to reach N by the probability that the ENP will still be present at that moment:

$$P\,(N) = 0.5\,N^{-0.5}\mathrm{e}^{-N/\Sigma}. \tag{14}$$

The average energy E_Σ is then obtained by the equation:

$$E_\Sigma = E_0 \int_1^\infty 0.5\,n^{0.5}\,\mathrm{e}^{-n/\Sigma}\,\mathrm{d}n. \tag{15}$$

Figure 11 compares the energies produced by ENPs that are stable and unstable. Figure 11 also shows that, although the average energy has a limit, some rare events are still possible yielding an amount of energy NE_0 even if N is larger than Σ. Figure 12 shows the relationship between Σ and E_Σ. Equation (15) is integrated via a numerical method.

We may conclude that the LENR energy created by an ENP depends on the number of reactions this particle triggers in the reactive lattice. In most cases, the number of reactions is limited to a value in the range of Σ. If we consider for example a surface power W of 1 W cm^{-2}, and $\Sigma = 10\,000$, the flux Φ of incoming ENPs should be:

$$\Phi = \frac{W}{E_0\Sigma}. \tag{16}$$

For $E_0 = 4$ MeV or 6.4×10^{-13} J, we obtain $\Phi = 1.5 \times 10^8$ ENPs cm^{-2} s^{-1}.

Some of the particles can trigger much more reactions than Σ. This may be the source of the craters. If Z_0 is different from zero, large series are frequent (Fig. 8). This does not reflect reality, otherwise craters would be the rule and their size would be larger than the few microns reported in the literature. Therefore, it should be concluded that ENPs, if they exist, react on the surface or at a very shallow depth.

Let us consider the case of $\Lambda = 50\,000$, and try to correlate the results with a typical 2 μm crater. Figure 7 shows that for this Λ value, the average of the squares of the excursions along the z-axis is 16 666. The square root of this value can be considered a measure of the penetration depth of the ENPs below the surface. This makes it possible to

make an estimation of the Mean Free Path:

$$\frac{Z_{\text{ave}}}{L} = \sqrt{16\,666} = 129 = 2{\times}10^{-6}\ \text{m/L}. \tag{17}$$

We obtain

$$L = \frac{2{\times}10^{-6}\text{m}}{129} = 155\ \text{Å}. \tag{18}$$

This estimation of the mean free path is an upper limit. If the crater is 2 μm in diameter, the Nuclear Active Environment responsible for its formation can only be smaller.

If we accept the time lapse of $\tau = 6$ ns for the formation of this 2 μm crater, we can derive the order of magnitude of the velocity U of the ENP travelling within the lattice:

$$50\,000\,L = \tau U = 775{\times}10^{-6}\text{m} = 6{\times}10^{-9}\text{s}\,U. \tag{19}$$

We obtain:

$$U = 129{\times}10^{3}\text{ms}^{-1}. \tag{20}$$

Other assumptions regarding the average energy E_0 per reaction would lead to different values of Σ, Λ, L, T and U. However, this would not change the overall behavior revealed by this simulation.

If ENPs exist and are the source of the phenomenon, and according to the assumptions considered in this simulation, we conclude that:

- The mean free path of ENPs in the metal is in the 100 Å range.
- The lifetime is in the nanosecond range.

7. Conclusion

If we take as a hypothesis that craters are created by a local burst of heat and that ENP are at the origin of the phenomena observed, a mathematical simulation leads to the following conclusions:

- The ENP reacts first at the surface or very close to the surface.
- The mean free path of the ENPs in the crystal structure is in the range of 100 Å.
- The ENP is not stable in the lattice and decays in about 1 ns.

This simulation alone cannot produce confirmation of the theories based on ENP. It can only give some clues concerning their properties in order for them to explain the experimental results.

Acknowledgments

The author thanks the referee for his very helpful comments and suggestions, and Jed Rothwell for his precious editorial assistance.

Appendix

A.1. Generation of Pseudo-random Numbers

The model requires the generation of three suites of random numbers comprised in the interval [0 – 1]. There are many algorithms available in the literature able to satisfy this need [17]. The theory shows that true randomness is

Table A1. Parameters used for the pseudo-random number generators.

	Multiplier M	Divider D
PRNG#1	16811	31
PRNG#2	29717	17
PRNG#3	24571	53

not achievable by algorithms. They are therefore described as Pseudo-random Number Generators (PSNG). John von Neumann wrote: "Anyone who considers arithmetical methods of producing random digits is, of course, in a state of sin." This problem is not critical, provided it is checked by statistical analysis that the PRNG suit the purpose of the intended use. In the present Monte-Carlo simulation, what is required is

(1) PRNGs with a distribution density sufficiently uniform across the [0 – 1] interval.
(2) Three PRNGs, each giving numbers which are independent from the two others.

The author decided to use his own generators, and test the results obtained according to these requirements. This experience proved interesting, so that it is briefly reported here, to show to the reader examples of potential traps, and as a testimony to von Neumann's words.

A.2. Algorithms Utilized

Most PRNGs are of the Linear Congruent type [18]. They are generally designed to generate pseudo-random numbers in large series, with a fast algorithm in order to minimize computation time. The general form is

$$X_{n+1} = (a\,X_n + c) \bmod m.$$

It can be demonstrated that the series generated have a period, dictated by the values of a and m. For details, see [18]. If $c = 0$, the generator is called a multiplicative congruential generator [18]. In the case of this study, the simulation was developed in Visual Basic, and the PRNGs had to use algorithms written in this language. The set of equations is

$$B = M\,X_n/D,$$

$$X_{n+1} = \mathrm{frac}\,(B)\,,$$

where frac(x) is the fractional part of x:

$$\mathrm{frac}\,(x) = \; x - \; \mathrm{integer}(x).$$

All numbers are defined in double precision and are calculated with 15 digits. *B* is an intermediate result. The value of the new iteration X_{n+1} is the fractional part of the intermediate number *B*. *M* is called the multiplier and *D* the divider. These numbers must be relatively prime in order to obtain a satisfactory randomness. Table A1 gives the values utilized for the simulation. All values in the table are prime numbers.

The value of *M/D* is large in order to get a uniform distribution of the values over the interval [0–1]. Following the intended use of the PRNG, different validity tests should be performed. In order to test the uniformity, 10^7 draws were made, and classified in 1000 bins between 0 and 1. The average number of draws per bin is 10 000.

The theoretical variance is

$$\sigma = \sqrt{10\,000} = 100.$$

Table A2. Test of uniformity of the independent PRNGs.

	Variance
PRNG#1	268.67
PRNG#2	108.90
PRNG#3	106.96

Table A3. Test of correlation between odd and even iterations.

	Variance
PRNG#1	63.26
PRNG#2	26.27
PRNG#3	56.39

The results of the test are listed in Table A2. We see that PRNG#1 is seriously flawed, while the others seem to pass this test.

An additional test is the correlation between successive odd and even iterations. The 10^7 draws are classified in a $100\times$ 100 grid. There should be 500 draws per cell, and the variance should be 22.36.

Another method to visualize the results is to plot the number of draws per cell using a false color code, as shown in Fig. 13. The color scale extends from mean –4 sigma (*dark red*) to mean +4 sigma (*violet*). In the case of a satisfactory test, the spots should appear as a shade of green, ranging from yellow–green to green–light blue.

Figure 13 proves that the three generators do not pass this test. Patterns are clearly visible on all pictures, and in the case of PRNG#1 and 3, the green is not the dominant color.

A known method to improve the randomness is to combine several generators [19]. This is the method followed here. The three generators are combined in a cyclic fashion, as follows:

$$X1_n = \text{frac}\left[M1/D1X1_{n-1} + LX3_{n-1}\right],$$

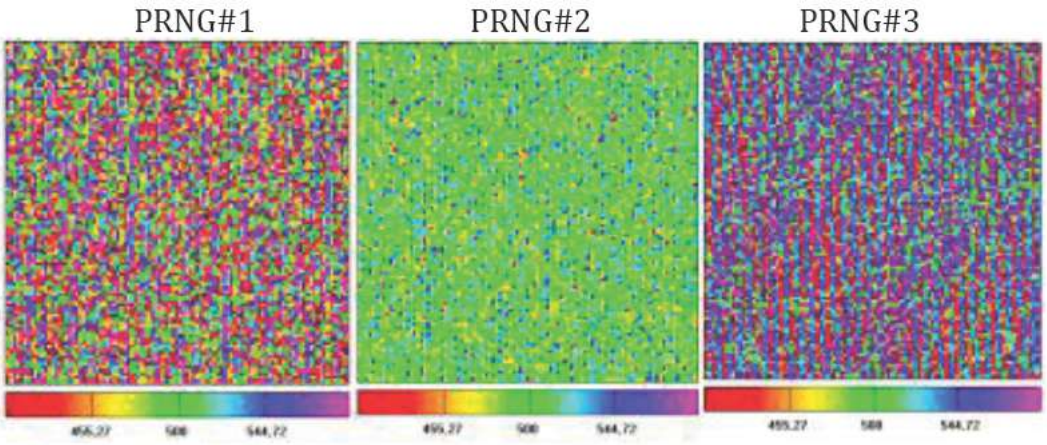

Figure 13. Correlation plots between odd and even iterations – 10^7 draws classified in 100 × 100 bins – Mean value per bin is 500 – sigma value is 22.36 – The color scale extends from mean –4 sigma = 410 (*dark red*) to mean +4 sigma = 589 (*violet*).

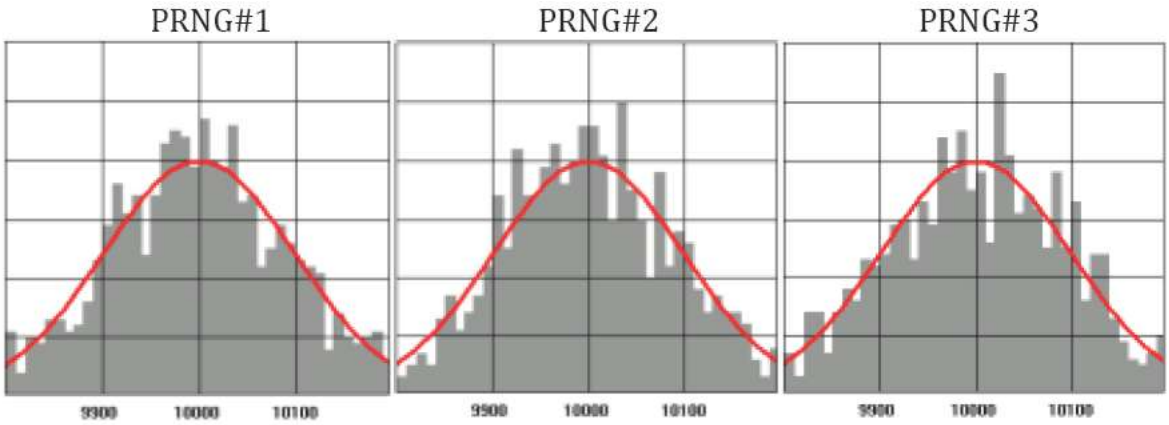

Figure 14. Histograms of the combined generators $-L = 3 - 10^7$ draws in 1000 bins – The red curves show the normal Gaussian distribution.

$$X2_n = \text{frac}\left[M2/D2X2_{n-1} + LX1_{n-1}\right],$$

$$X3_n = \text{frac}\left[M3/D3X3_{n-1} + LX2_{n-1}\right],$$

where L is a positive number called link L values different from zero improve the results of the uniformity test. All PRNGs passed this test with L larger than 1. Figure 14 shows the histograms of the combined generators with a link $L = 3$. Comparison of the histograms with the normal Gaussian distribution (*red curves*) shows that the statistical distribution is satisfactory.

Figure 15 shows the influence of L on the correlation test results. The three generators are considered acceptable and suited for the simulation with $L = 3$. The correlation test is satisfied if $L > 1$.

The color plots are reproduced in Fig. 16. The main color is now green. The generators are now linked via L. It is therefore necessary to check that they are not correlated. A similar procedure was followed to test the correlation

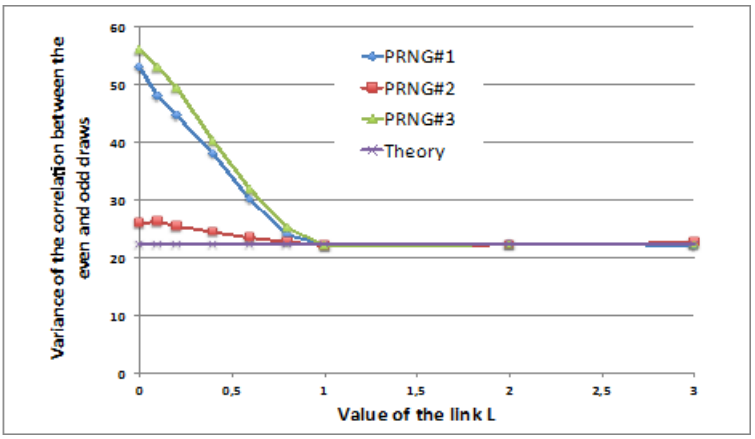

Figure 15. Influence of L on the variance of the correlation tests.

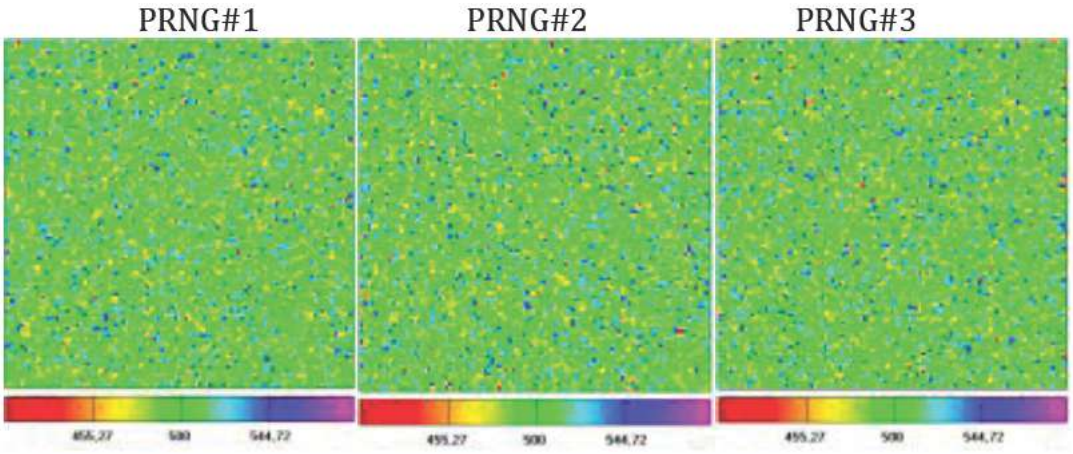

Figure 16. Color plots of the correlation plots test between odd and even iterations – 10^7 draws classified in 100 × 100 bins – Theoretical mean value per bin is 500 – Theoretical sigma value is 22.36 – The color scale extends from mean –4 sigma = 410 (*dark red*) to mean +4 sigma = 589 (*violet*).

between pairs of draws. Figure 17 shows the color plots and the variance of the different couples. The test is made with 10^7 draws classified in 100× 100 bins. The mean number per cell is 1000 and the theoretical variance is: $\sigma = 31.62$. We see that the generators are not statistically correlated.

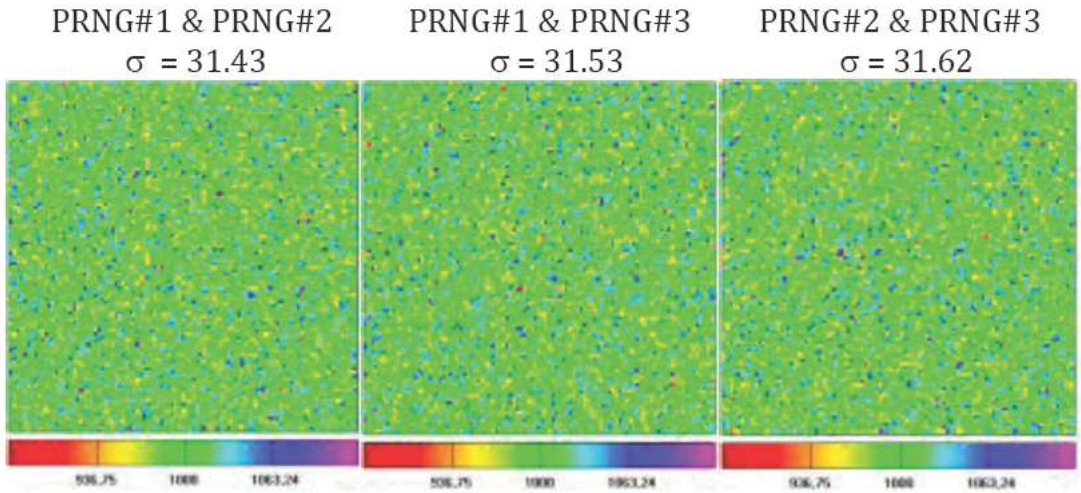

Figure 17. Correlation plots of couples of generators – 10^7 draws classified in 100 × 100 bins – Theoretical mean value per bin is 1000 – Theoretical sigma value is 31.62 – The color scale extends from mean -4 sigma = 874 (*dark red*) to mean +4 sigma = 1126 (*violet*).

A.3. Conclusion

This study shows that the PRNGs considered are suitable for the model used in this paper. They generate numbers uniformly distributed, and no statistical correlation is detected between the three generators. It is also shown that the random behavior desired might not be obtained in the first attempt, and that a thorough statistical analysis is necessary.

References

[1] E. Storms, *The Explanation of Low Energy Nuclear Reaction*, Infinite Energy Press, ISBN 978-1-892925-10-7 (2014).
[2] V.A. Chechin, V.A. Tsarev, M. Rabinowitz and Y.E. Kim, Critical review of theoretical models for anomalous effects in deuterated metals, *Int. J. Theoret. Phys*. **33** (1994) 617–670.
[3] J.C. Fisher, Poly-neutrons as agents for Cold Fusion reactions, *Fusion Technol.* **22** (1992) 511.
[4] J.C. Fisher, Neutron isotope theory of LENR process, *J. Condensed Matter Nucl. Sci.* **15** (2015) 183–189.
[5] Y.N. Bazhutov, Erzion model features in cold nuclear transmutation experiments, *Proc. 8th Int. Workshop on Anomalies in Hydrogen/Deuterium Loaded Metals*, pp.12–18, www.iscmns.org/catania07/procw8.
[6] Y.N. Bazhutov, Erzion model interpretation of the experiments with hydrogen loading of various metals, preprint of ICCF 17, *J. Condensed Matter Nucl. Sci.* **13** (2014) 29–37.
[7] W. Collis, Nuclear reactions of cold fusion – a systematic study, *Proc ICCF5,* Monte Carlo.
[8] W. Collis, ENSAP software tool to analyse nuclear reactions, in *The Seventh Int. Conf. on Cold Fusion,* 1998, Vancouver, Canada: ENECO Inc., Salt Lake City, UT.
[9] W. Collis, Improving the Erzion model, *Book of abstracts of the 8th Int. Workshop on Anomalies in Hydrogen/Deuterium Loaded Metals*.
[10] S. Szpak, P.A. Mosier-Boss and F.E. Gordon, Experimental evidence for LENR in a polarized Pd/D lattice, NDIA 2006 Naval S&T Partnership Conference, Washington DC, http://lenr-canr.org/acrobat/SzpakSexperiment.pdf.
[11] David J. Nagel, Characteristics and energetics of craters in LENR experimental materials, *J. Condensed Matter Nucl. Sci.* **10** (2013) 1–14.
[12] J. Ruer, Simulation of crater formation on LENR cathodes surfaces, *J. Condensed Matter Nucl. Sci.* **12** (2013) 1–16.
[13] https://en.wikipedia.org/wiki/Mean_free_path.
[14] https://en.wikipedia.org/wiki/Brownian_motion.
[15] https://fr.wikipedia.org/wiki/Mouvement_brownien.
[16] https://en.wikipedia.org/wiki/Fick%27s_laws_of_diffusion.
[17] https://en.wikipedia.org/wiki/Pseudorandom_number_generator.
[18] https://en.wikipedia.org/wiki/Linear_congruential_generator.
[19] https://en.wikipedia.org/wiki/Combined_Linear_Congruential_Generator.